Molecular Omics

ROYAL SOCIETY OF CHEMISTRY

RESEARCH ARTICLE

View Article Online
View Journal | View Issue

Cite this: *Mol. Omics*, 2023, **19**, 552

Butyrate promotes C2C12 myoblast proliferation by activating ERK/MAPK pathway†

Li Guan,‡[a] Ziyi Cao,‡[a] Ziyue Pan,[b] Chao Zhao,[c] Mengjuan Xue,[d] Fan Yang*[e] and Jie Chen*[a]

Received 3rd October 2022,
Accepted 19th April 2023

DOI: 10.1039/d2mo00256f

rsc.li/molomics

Sarcopenia has garnered considerable interest in recent years as ageing-associated diseases constitute a significant worldwide public health burden. Nutritional supplements have received much attention as potential tools for managing sarcopenia. However, the specific nutrients responsible are still under-investigated. In the current study, we first determined the levels of short chain fatty acids (SCFAs) and intestinal flora in the feces of elderly sarcopenia subjects and elderly healthy individuals by ultra-performance liquid chromatography tandem mass spectrometry (UPLC-MS/MS). Then cell viability detection, flow cytometry and transcriptome analysis were adopted to experimentally evaluate the effect and the underlying mechanism of SCFA on C2C12 cells proliferation *in vitro*. The results suggested that patients with sarcopenia exhibited decreased levels of butyrate. And butyrate may stimulate C2C12 myocyte proliferation *via* promoting G1/S cell cycle transition. Transcriptomic analyses pointed to upregulation of the Mitogen-activated protein kinase (MAPK) signaling pathway in butyrate-treated cells. In addition, the above proliferative phenotypes could be suppressed by the combination of ERK/MAPK inhibitor. A combined transcriptomic and metabolomic approach was applied in our study to investigate the potential effect of microbiota-derived butyrate yield on muscular proliferation which may indicate a protective effect of nutritional supplements.

Introduction

Sarcopenia is an aging-associated muscle atrophy characterized by functional decline due to muscle anabolism alteration and regeneration abnormalities. Muscle stem cells, also known as muscle satellite cells (SC) are essential for muscle regeneration through arousal, proliferation, and subsequent differentiation after injury.[1] However, elevated pSmad3 and decreased Notch activation, associated with muscle SC aging, reduce the regenerative capacity.[2] Several nutrients can boost the anabolic metabolism of skeletal muscle fibers through intestinal microorganisms and metabolites. However, the specific factors promoting muscle regeneration abnormalities in the elderly are unknown. Besides, the role of nutritional factors and certain metabolites in regulating the myocyte self-renewal capacity is promising and should be assessed.

Short-chain fatty acids (SCFAs) refer to organic fatty acids with less than 6 carbon atoms in the carbon chain, mainly including acetic acid, propionic acid and butyric acid.[3] The SCFAs directly obtained by the human body from food are very limited.[3] SCFAs are mainly from the digestion of some indigestible carbohydrates by intestinal microflora, such as resistant starch and dietary fiber.[4] Because short-chain fatty acids are mainly produced by intestinal microflora, factors affecting intestinal microflora, such as the use of antibiotics, modern sanitation facilities, diet quality and environmental factors, and lifestyle can all affect the production of SCFAs.[5–7] At present, many studies focus on the relationship between intestinal flora, short chain fatty acids and sarcopenia.

Butyrate is one of the SCFAs. Firmicute is considered to contribute most to butyrate production.[8] Butyrate producing Firmcute species that are particularly prevalent in the colon include Faecalibacterium prausnitzii, Eubacterium rectale and Roseburia intestinalis.[9] Butyrate has extensive effects on the body like other SCFAs and the bioactivities of which are related to inhibition of class I and class II histone deacetylases.[10]

In recent years, many studies have reported that butyrate is closely related to muscle function. Butyrate can modulate myocardial tissue restoration by inhibiting the enzyme histone deacetylase.[11] Butyrate can attenuate oxidative stress and

[a] *Department of Gastroenterology, Huadong Hospital affiliated to Fudan University, Shanghai, China. E-mail: laugh_chenjie@fudan.edu.cn*
[b] *Department of Gastroenterology, Minhang Hospital affiliated to Fudan University, Shanghai, China*
[c] *Key Laboratory of Medical Molecular Virology, School of Basic Medical sciences, Shanghai Medical College, Fudan university, Shanghai, China*
[d] *Department of Endocrine, Huadong Hospital affiliated to Fudan University, Shanghai, China*
[e] *Shanghai Key laboratory of Clinical Geriatric Medicine, Shanghai, China. E-mail: fdyangfan@fudan.edu.cn*

† Electronic supplementary information (ESI) available. See DOI: https://doi.org/10.1039/d2mo00256f

‡ These authors contributed equally to this article.

apoptosis to alleviate age-related skeleton muscle atrophy in mice.[12] Butyrate can affect glucose metabolism in muscle cells through activation of AMPK signal pathway and mitochondrial fatty acid oxidation stimulation.[13–15] Several studies have demonstrated that butyrate functions through insulin-stimulated glucose uptake enhancement and intramuscular lipid deposition attenuation, thus improving muscle mass and function.[12,16] GPR41/GPR43, expressed on myocytes serving as SCFA receptors, mediate the effects of butyrate on skeleton muscle cells.[17,18] Existing studies have shown the complex effects of butyrate on muscle tissue, but the role of butyrate in myoblast proliferation is still unclear. This study aimed to evaluate the effect of butyrate on myocyte regeneration and the possible mechanism, which may provide a new perspective for the treatment of sarcopenia.

Intestinal microflora is closely related to metabolism. The joint study of microbiome and metabolome is considered to be the most promising method to evaluate host microbiome interaction. Our team first detected the intestinal metabolites and gut microbiota in the elderly sarcopenia population and found that the level of butyrate decreased. Then, C2C12 cell line was used to verify that butyrate could promote proliferation through the ERK signaling pathway *in vitro*. To some extent, it indicates the possibility of butyrate for improving sarcopenia.

Experimental

Subjects

This study included 15 subjects who underwent sarcopenia evaluation in November 2020, among which there were 5 males, 10 females, 7 sarcopenia and 8 non sarcopenia. The exclusion criteria were: prolonged bed rest with the inability to independently move and acute or severe illnesses, such as fever, dehydration, and cardiopulmonary disease, *etc.* This study followed the Huadong Hospital regulations, and the Ethics Committee approved all procedures of Huadong Hospital, Fudan University (20190068).

The AWGS 2019 diagnostic algorithm was used to define sarcopenia. Physical function was evaluated by timing a 6 m gait speed. A 6 m walk speed less than 1 m s^{-1} was considered as low physical performance. The body composition analyzer (Inbody 270, Inbody Inc., Tokyo, Japan) was used to assess the appendicular skeletal muscle mass (ASM). The ASM index (ASMI) was calculated as the ratio of ASM and squared height. The ASMI-cutoff points were set as 7.0 kg m^{-2} for men and 5.7 kg m^{-2} for women to define muscle mass degeneration. The grip strength meter was used to measure the grip strength.

Metabolite detection

Fecal samples were obtained from 15 admitted subjects for further metabolite extraction and detection. Informed consent was also obtained from the patients. All the samples were stored at −80 °C, after submission to Metabo-Profile Biotechnology (Shanghai) Co., Ltd for UPLC MS/MS-based metabolomics analysis using Q300 kit. The raw data files generated by UPLC-MS/MS were processed using MassLynx software (v 4.1, Waters Corp., Milford, MA, USA) for peak integration, calibration, and quantification of each metabolite. The self-developed platform iMAP (v1.0, Metabo-Profile, Shanghai, China) was used for statistical analysis.

Detection of intestinal flora

According to the instruction of E.Z.N.A ® DNA kit (Omega Bio-tek, Norcross, GA, US), the total genomic DNA of the microbial community was extracted and DNA concentration was measured using NanoDrop2000 (Thermo Scientific company, USA). The v3–v4 variable region of the 16S rRNA gene was PCR amplified using the extracted DNA as a template. 3 replicates per sample. After mixing the PCR products of the same sample, 2% agarose gel was used to recover the PCR products. The recovered products were purified by the AxyPrep DNA Gel Extraction kit (Axygen Biosciences, Union City, CA, USA) and was quantified by quantum™ Fluorometer (Promega, USA). Illumina MiSeq (Illumina, San Diego, CA, USA) high-throughput sequencing was completed by Shanghai Meiji Biomedical Technology Co., Ltd. The data were analyzed on the online platform of Majorbio Cloud Platform (**https://www.majorbio.com**).

Cell culture

The C2C12 murine myoblast cells were obtained from the FuHeng Biology (Shanghai, China). The C2C12 myoblasts was passaged once or twice for further experiments. The proliferating myocytes were cultured in a growth medium (DMEM, Corning) containing 10% fetal bovine serum and 1% penicillin–streptomycin liquid (Thermo Fisher Scientific) at 37 °C and 5% CO_2. Sodium butyrate treatment was performed at 750 μM concentration and U0126 at 10 and 20 μM concentration for 48 h. The control group of this study is sodium chloride solution with corresponding sodium concentration. Sodium butyrate was purchased from Aladdin (Shanghai, China) and U0126-EtOH (HY-12031) from MCE.

CCK-8 assay

A CCK8 kit (CK04, Dojindo, Japan) monitored cell viability following the manufacturer's instructions. The C2C12 cells treated with butyrate or U0126 (2000 cells per well) were cultivated in 96-well plates with five replicate wells. A CCK-8 solution (10 μl) was added to each well. Sterile PBS was then added to the surrounding wells to prevent evaporation. A microplate reader was used to measure the absorbance at 450 nm after one hour of incubation.

Cell cycle analysis

The cell cycle distribution was analyzed using propidium iodide (PI)/RNAse staining for flow cytometry. After trypsin digestion of the adherent C2C12 myoblast, the cells were collected and gently washed with PBS. Cell pellets were obtained by centrifugation at 1000 rpm for 3 min and then resuspended in pre-chilled 75% ethanol, fixed at 4 °C for at least 24 h. FxCycle PI/RNase staining solution (F10797, Thermo Scientific) was applied to fixed cells at room temperature for 30 min at dark

ambient. Finally, the cells were subjected to cytometry assay and FlowJo software was used for analysis of cytometric data.

Immunofluorescence staining

The treated cells were washed twice using PBS, then fixed with 4% paraformaldehyde and permeabilized with 0.3% Triton X-100, 10% goat serum in PBS. The cells were then incubated with primary antibodies prepared using blocking buffer at 4 °C overnight, followed by incubation with conjugated secondary antibodies at room temperature for 2 h. The cells were then counterstained using Hoechst 33342 dye. Each staining was followed by extensive PBS washing. Eight fields of view were randomly selected at 40× magnification for each confocal dish, and images were captured using a laser confocal microscope (SP5, Leica).

Transcriptomic sequencing analysis

C2C12 cells were divided into two groups ($n = 3$), one group was treated with butyrate, and the other group was used as control. After 48 h treatment, cells were lysed with Trizol, and the RNA of cells was extracted. Transcriptomic sequencing analysis was performed through the Illumina sequencing platform. The transcriptome results were subsequently analyzed using R. The R packages of ClusterProfiler and org.Mm.eg.db were applied for GO and KEGG analysis. The ggplot2 package was used for the visualization of the results.

Western blotting

The cell lysates were prepared using RIPA lysis buffer (P0013B, Beyotime) containing 1 mM PMSF and phosphatase inhibitors (88667, Thermo Scientific) on ice for total protein extraction after 48 h of cell culture. The BCA assay kit was used to quantify the extracted proteins, then they were mixed with SDS loading buffer and denatured at 100 °C for 15 min. The mixture underwent 5 min of centrifugation at 5000 g at 4 °C, then the protein supernatants were subjected to SDS-polyacrylamide gel electrophoresis for separation and then transferred to nitrocellulose. The ECL system was used to detect the immunoreactive band signal, then visualized using the BioRad imager system. See Table S1 (ESI†) for antibody information and dilution ratio of each antibody.

RNA extraction and real-time PCR

Cell Lysis Buffer (EZBioscience, USA) was used to extract the total RNA of C2C12 myoblast following the manufacturer's instructions. The cDNA was synthesized through polymerase chain reaction amplification using the PrimeScript™ RT Master Mix (Takara Bio, Shiga, Japan) on a thermal cycler apparatus (Applied B PE4500, USA) and stored at 4 °C for expression level evaluation. One Step SYBR® PrimeScript™ RT-PCR Kit II (TaKaRa, China) was used for subsequent quantitative real-time RT-PCR (Qrt-PCR) in a 20 μl reaction.

The primers used in the real-time PCR are shown in Table S2 (ESI†).

Statistical analysis

Each experiment was performed at least three times. The statistical significance of the results was determined using GraphPad Prism 7 and SPSS 20.0 through Student's *t*-test or chi-square test. A value of $P < 0.05$ was considered statistically significant.

Results

The fecal butyrate content of sarcopenia patients decreased significantly

As shown in the Table 1, there was no statistically significant difference in age, gender, or body mass index (BMI) between the healthy control and the sarcopenia subjects, while appendicular skeletal muscle mass (ASM) and physical performance, such as grip strength and 6 m gait speed (GS) were decreased in sarcopenia patients.

The fecal samples of eight healthy elderly people and seven sarcopenia patients were collected, and the levels of metabolites were measured. Through the quantitative detection of fecal metabolites of each sample, we found that SCFAs ($p = 0.02$) and nucleotides ($p = 0.04$) decreased in the sarcopenia group (Fig. 1A). This study focused on the role of SCFAs in sarcopenia. Further analysis of changes in SCFAs showed that the levels of butyric acid and acetic acid significantly decreased (Fig. 1B). Levels of other short-chain fatty acids were not significantly different (Fig. 1B). This mainly explored and verified the pathological mechanism of butyric acid involved in sarcopenia. We subsequently made a correlation analysis between butyrate and age, BMI, ASM, grip and 6 m gait speed (GS). We found butyrate content was negatively correlated with age (Fig. 1B) and positively correlated with BMI, ASM, grip and 6 m gait speed (Fig. 1C–G). Among them, the correlation between butyrate and ASM, grip, 6 m gait speed were statistically significant ($p < 0.05$).

Changes of intestinal microflora composition in subjects with sarcopenia

The level of metabolites in the intestine is closely related to the intestinal flora, so we also examined the composition of intestinal flora in normal elderly people and sarcopenia patients. α-Diversity is an indicator of taxonomic diversity within a sample, which was measured by Shannon index and

Table 1 Clinical characteristics of participants

	Mean ± standard deviation		
Clinical parameters	Without sarcopenia ($n = 8$, female = 5)	With sarcopenia ($n = 7$, female = 5)	*p*-value
Age (years)	69.38 ± 6.84	72.00 ± 10.68	>0.05
BMI (kg m^{-2})	22.96 ± 2.33	20.77 ± 2.32	>0.05
ASM (kg)	18.10 ± 3.66	14.17 ± 1.73	<0.05
ASMI (kg m^{-2})	6.63 ± 0.84	5.70 ± 0.63	<0.05
Grip (kg)	31.44 ± 8.13	22.00 ± 6.25	<0.05
6 m gait speed (m s^{-1})	1.28 ± 0.18	1.02 ± 0.21	<0.05

Abbreviations: BMI, body mass index; ASM, appendicular skeletal muscle mass; ASMI, appendicular skeletal muscle index.

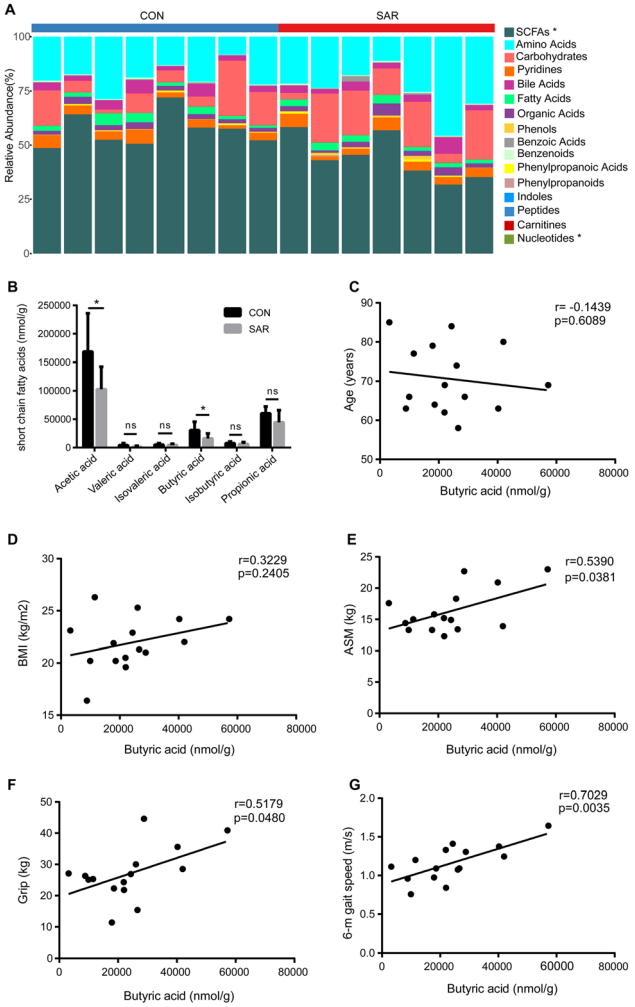

Fig. 1 The content of the fecal butyrate decreased in sarcopenia subjects. (A) The levels of metabolites in each sample. (B) The levels of SCFAs in healthy controls and sarcopenia subjects. (C) Correlation analysis between butyrate content and age. (D) Correlation analysis between butyrate content and body mass index (BMI). (E) Correlation analysis between butyrate content and appendicular skeletal muscle mass (ASM). (F) Correlation analysis between butyrate content and grip. (G) Correlation analysis between butyrate content and 6 m gait speed.

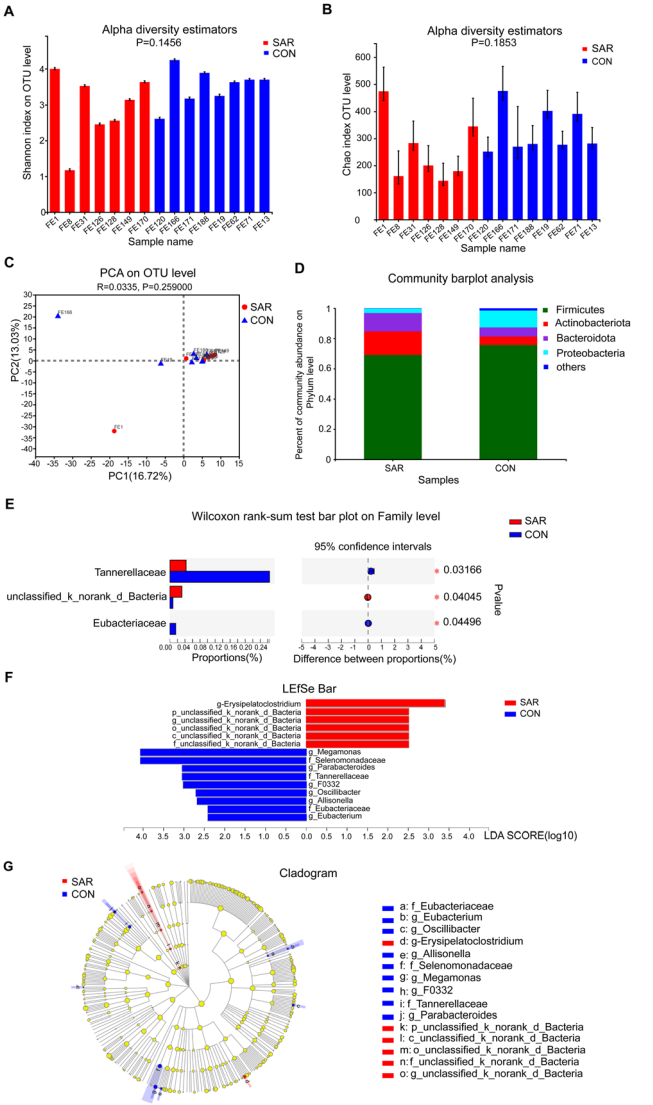

Fig. 2 Changes of intestinal microflora composition in sarcopenia subjects. (A) Shannon index analysis. (B) Chao index analysis. (C) Beta diversity analysis. (D) Community abundance on phylum level of healthy controls and sarcopenia subjects. (E) Species difference analysis on family level. (F and G) LEfSe analysis on genus level.

the Chao index. We determined that the Shannon effective index as well as the Chao index were not significantly different in sarcopenia patients *vs.* healthy subjects (Fig. 2A and B). Next, the microbial community structure (β- diversity) was assessed using ANOSIM (analysis of similarities). The results showed that these differences were subtle and there was no obvious clustering of samples (Fig. 2C). In both healthy control and sarcopenia groups, Firmicutes was the most abundant phylum of bacteria. Compared with the healthy control group, the abundance of Firmicutes and Proteobacteria in sarcopenia patients decreased, while the proportion of actinobacteria and bacteroidota increased,but with no statistical difference (Fig. 2D). At the family level, Tannerellaceae, unclassifiied_k__norank_d__Bacteria, Eubacteriaceae were significantly decreased in sarcopenia group ($p < 0.05$) (Fig. 2E). In addition, at the genus level, we used Lefse (linear discriminant analysis, LDA = 2) to analyze differentially abundant taxa of sarcopenia. This result shows a difference of g__ Erysipelatoclostridium has the greatest impact on sarcopenia (Fig. 2F and G).

Butyrate promotes the proliferation of C2C12 myoblast cells

The above analysis suggests that there may be a close relationship between butyrate and skeletal muscle function. In order to further verify the role of butyrate, we used cell lines for experimental verification. C2C12 cells are a myoblast cell line derived from murine satellite cells and are commonly used as an *in vitro* model of muscle regeneration. Therefore, C2C12 cell line was used in subsequent experiments. Myoblast proliferation is the most crucial initial step in myogenesis progression. Herein, the C2C12 cells were treated with 750 μM butyrate for 24 h and 48 h, then CCK-8 assay was used to observe the

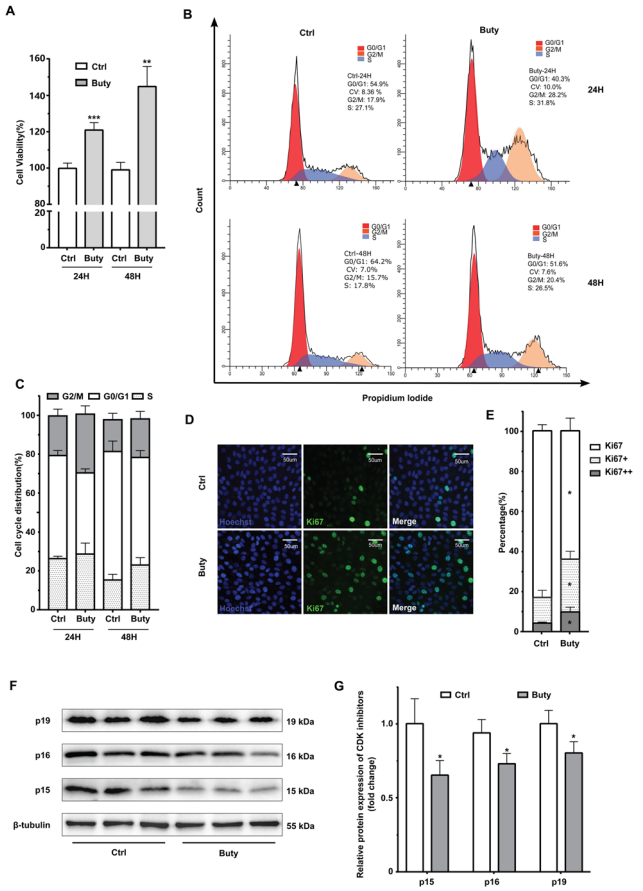

Fig. 3 Butyrate promotes C2C12 myoblast proliferation. (A) Cell viability assessed at 24 h and 48 h after butyrate treatment using the CCK-8 assay ($n \geq 3$); (B) representative FACS histograms of the cell cycle analysis using flow cytometry at 24 h and 48 h; (C) quantification of cell population in different cell-cycle phases. (D) representative fluorescence images. Total C2C12 myoblast nuclei were visualized using Hoechst staining (blue), and the proliferating ones were visualized with Ki67 (green). (E) Quantification of the percentage of Ki67-positive myoblasts (3 wells per group, 5 random fields per well). Scale bars = 50 μm; (F) representative immunoreactive bands of p16, p19, and β-tubulin. (G) Quantification of the expression level of cell cycle-related proteins. ***$P < 0.001$; **$P < 0.01$; *$P < 0.05$; NS nonsignificant.

proliferous effect. Butyrate treatment significantly increased the cellular proliferation activity and viability (Fig. 3A).

The cell cycle, subdivided into various phases, plays a key role in cell proliferation. Flow cytometry was used further to explore the underlying mechanism for butyrate-induced myoblast growth.

Butyrate-treated cells showed an increased S-phase cell population accompanied by simultaneous decrease in G1 phase population. In particular, the S-phase cell population significantly increased after 48 h of butyrate treatment, indicating the best proliferous effect (Fig. 3B and C).

The myoblast cells were stained using Ki67 and graded as Ki67++, Ki67+, and Ki67-according to the intensity of immunostaining to quantify the proliferation rate. The Hoechst-positive and Ki67-positive nuclei were then scored. The percentage of Ki67+ and Ki67++ nuclei in the butyrate-treated C2C12 myoblast

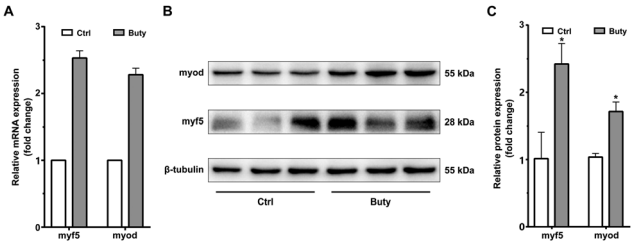

Fig. 4 Butyrate enhances the expression of the early myogenic factors in C2C12 cells. (A) Relative mRNA expression level analyzed using Real-Time PCR and normalized to tubulin mRNA. (B) Representative western blot of MRFs detected at 48 h after butyrate administration. (C) Quantification of the expression of MRFs protein normalized to the β-tubulin. **$P < 0.01$; *$P < 0.05$.

was significantly increased, while the percentage of Ki67- nuclei was decreased (Fig. 3D and E).

The expression of cell cycle regulators, such as p16, p19, and p15, was also analyzed to validate the flow-cytometric assay results. The expression of p15, p16, and p19 substantially decreased after butyrate treatment for 48 h (Fig. 3F and G).

Sodium butyrate enhances the expression of the early myogenic factors in C2C12 cells is at the proliferating phase

Myogenesis is a multi-factorial process, which is highly coordinated and driven by various myogenic regulators. The activation of muscle-specific promyogenic factors expressed at the early steps of the myogenic process is crucial in myogenesis. This study quantified the expression level of Myf-5 and MyoD after treatment with butyrate. The Myf5 and MyoD were upregulated in C2C12 cells at the mRNA and protein levels (Fig. 4A–C). These MRFs above play a key role in initiating the onset of the differentiation stage.

Butyrate enriches the MAPK signaling pathway in the butyrate-treated C2C12 cells

Transcriptomic profiling was conducted to examine the gene expression changes induced by butyrate treatment in the C2C12 myoblast proliferous stage. The generated data were subjected to bioinformatic analysis.

A total of 1688 differentially expressed genes (DEGs) (1311 genes (blue) were upregulated and 357 genes (red) were downregulated) were identified using the following screening criteria: adjusted $P < 0.05$ and $|\log \mathrm{FC}| > 1$. These DEGs were displayed as the heatmap and the volcano plot using the ggplot2 package of R language (Fig. 5A and B).

We selected some DEGs of interest for Gene Ontology (GO) annotation analysis. In Fig. 5C, genes were associated with the wound heeling, ERK cascade regulation, myoblast fusion and so on. DEGs were then subjected to KEGG enrichment analysis to further investigate their roles. KEGG analysis revealed that these genes were enriched in the proliferation-related pathways, including the MAPK, PI3K–Akt pathway (Fig. 5D). The above results indicated that the promoting effect of butyrate on C2C12 cells may be related to the MAPK/ERK pathway.

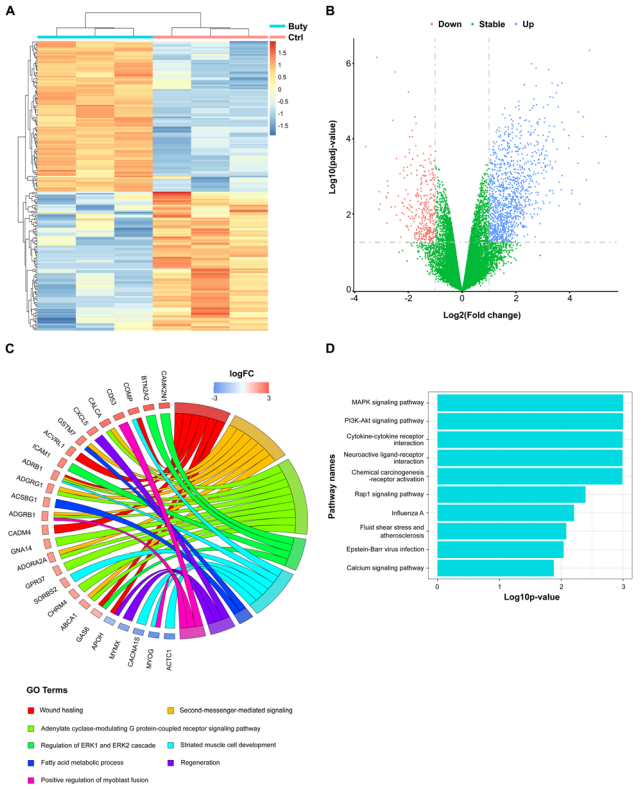

Fig. 5 Transcriptome analysis of C2C12 cells treated with butyrate. (A) The heatmap display of differentially expressed genes (DEGs) of control group and butyrate treated group. (B) The volcano map display of DEGs of control group and butyrate treated group. (C) Chord plot showing a selection of GO terms connecting DEGs. D. KEGG enrichment analysis with top 10 pathways.

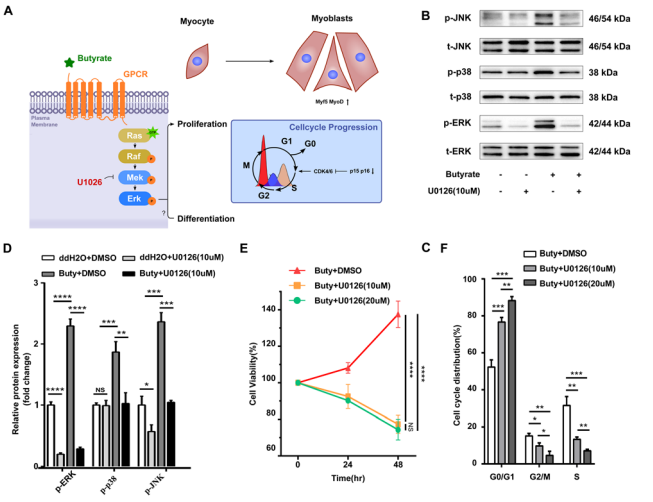

Fig. 6 ERK Inhibitor U0126 reverses the proliferative effect induced by butyrate. (A) Schematic illustration of butyrate-induced ERK signaling activation and myocyte proliferation; (B) representative western blot of ERK-related pathways determined through western blot analyses; (C) quantification of the level of ERK-related pathway phosphorylation. (D) Cell viability detected at 24 h and 48 h after butyrate and U0126 co-treatment using the CCK-8 assay; (E) quantification of cell population in different cell-cycle phases. ****$P < 0.0001$; ***$P < 0.001$; **$P < 0.01$; *$P < 0.05$; NS nonsignificant.

ERK inhibitor significantly suppresses the effect of butyrate on the proliferation and cell cycle

The ERK1/2 are key promoters of myoblast proliferation.[19] Therefore, butyrate could be promoting C2C12 myoblast proliferation by upregulating ERK phosphorylation. Herein, a combination of U0126 (10 μM and 20 μM), a well-established ERK pathway inhibitor, and butyrate (750 μM) was administrated to the proliferating C2C12 cells for 24 h and 48 h to validate the above hypothesis.

The ERK and related pathways were subjected to immunoblotting for inhibitor validation. western blot analysis of ERK-related pathways indicated that the activation of signaling pathways reflected by the increase in phosphorylation levels of ERK was reversed after U0126 administration (Fig. 6B and C).

The C2C12 myoblast was treated with U0126 after cell proliferation detection using CCK-8 assays to validate the roles of the ERK signaling pathways in driving myoblast proliferation. The U0126 co-treatment inhibited the increased cellular viability mediated by butyrate (Fig. 6D). In cell-cycle distribution analysis using flow cytometry, C2C12 cells cotreated with butyrate and U0126 yielded results consistent with those obtained using CCK-8 (Fig. 6E).

Taken together, these results indicate that butyrate promotes C2C12 proliferation through the ERK pathway.

Discussion

Aging-associated diseases are a worldwide public health burden due to the increased aging population in developed and developing countries. As a result, sarcopenia has attracted much interest due to its association with constrained physical activity, increased risk of falls, and high healthcare costs.[20,21] The clinical interventions targeting various populations with sarcopenia are under extensive discussion. Currently, resistance exercise is the main treatment option for sarcopenia. Nevertheless, nutritional status, such as low BMI and malnutrition, are associated with a higher risk of sarcopenia, indicating that nutrition-reserve oriented intervention can prevent and treat age-specific muscle mass and function decline.[22,23]

This study detected a descender of fecal butyrate, one of the key SCFAs associated with muscle regeneration, in elderly sarcopenic individuals (Fig. 1A and B). Butyrate, as an energy substance, provides energy for colonocytes. Hence, the effect of butyrate on muscular tissue should be further assessed.[24] Through the correlation analysis between butyrate and clinical data of patients, the results show that butyrate is closely related to skeletal muscle quality and function (Fig. 1C–G). Recent studies have shown that there is a complex interaction between gut microbiota and fragile muscles through the microbial metabolites.[13,25,26] Studies have shown that frailer individuals reduce butyrate producing bacteria, such as Faecalibacterium prausnitzii.[27] Thus we also examined the intestinal flora of patients with sarcopenia. However, we found no difference in overall microbial diversity (Fig. 2A–D). While at the family level, we detected that the level of Eubacteriaceae in sarcopenia patients decreased (Fig. 2E), and the Eubacteriaceae is one of

the producers of butyrate.[28,29] This may explain the decreased intestinal butyrate level in sarcopenia patients. In the genus level, Erysipelatoclostridium was considered to be the bacterium most closely related to sarcopenia through the Lefse analysis (Fig. 2F and G). However, the relationship between Erysipelatoclostridium and skeletal muscle has not been reported in the literature. In fact, prior to this, there had been a larger clinical study that found a decrease in intestinal microflora diversity and butyrate levels in patients with sarcopenia,[30] which also validated our results. On this basis, our team further explored the specific mechanism of butyrate on myoblasts.

Our study showed that butyrate can enhance skeleton muscle regeneration (Fig. 3). Herein, the expression of myogenic regulatory factors was significantly increased in C2C12 myoblasts, including Myf5 and MyoD (Fig. 4). The expression of early myogenic regulatory factors, Myf5 and MyoD, regulate muscle satellite cell activation.[31] For instance, decreased Myf5 expression can delay and decrease regeneration of injured muscle.[32,33] Although the modulatory action of Myf5 in skeletal myoblast proliferation rate is known, this study did not find a conclusive modulatory action, and thus further validation is required.[34]

Satellite cell activation and proliferation upon injury are crucial in aging-related muscular regeneration. Therefore, they are potential therapeutic targets for sarcopenic patients.[35] MAPK signaling pathways regulate cellular fate in various cells by altering pleiotropic cellular functions. In particular, MAPK signaling underlies multiple aspects, including cell viability, proliferation, differentiation, and protein degradation in myocytes.[36–38] The PA-induced glucose uptake in C2C12 cells is repressed through the blockade of the ERK1/2 activity.[39]

Extensive research has shown that the activated ERK/MAPK activates the expression of target genes essential for proliferation in multiple cells. In our research, we performed transcriptomic analysis on C2C12 cells treated with butyric acid. The results showed that the elevated GPCR signaling level mediated butyrate-induced ERK/MAPK activation since GPCR41/43 acts as SCFA receptors (Fig. 5). And this study also used CCK-8 assay and cell cycle distribution analysis to verify the proliferous effect of the ERK pathway in multiplying C2C12 myoblast cells[19] (Fig. 6).

Although our experimental results prove the promoting effect of butyrate on myocytes to a certain extent, our research still has certain limitations. We consider that the sample size included in the study may be too small, and subsequent studies need to be verified in a larger population sample. Moreover, further research with strong serological data and large population is required to determine the relationship between butyrate and sarcopenia or to develop such a multidimensional biomarker. And this study mainly explored the possible role of intestinal metabolites in sarcopenia, so it did not go further in the relationship between intestinal bacteria and sarcopenia. In addition, this study only verified the myogenic effect of butyrate *in vitro*, lacking the *in vivo* level, and further demonstration is needed in subsequent experiments.

Researchers can use metabolomics to assess the potential biomarkers for various diseases to explain the role of intestinal bacteria and their metabolites in the development of debilitating diseases. Therefore, future studies may provide novel and personalized therapeutic approaches for various diseases. Fructan-based dietary prebiotic or resistant potato starch (RPS) supplementation can modulate the relative abundance of specific butyrogenic bacteria and butyrate production.[40] Furthermore, prebiotics, such as inulin-type fructans (ITF) and arabinoxylan-oligosaccharides (AXOS), are beneficial for the interaction between bifidobacteria and butyrate-producing bacteria, thus improving yield. Although prebiotics can improve the abundance of certain bacteria, combined approaches using nutrition and exercise, such as ''add-on'' therapies, are recommended to promote the rejuvenation of intestinal microbiota structure in the frail elderly.[41]

Conclusions

This is the first study to combine transcript profiling and metabolomic analysis to show that microbiota-derived butyrate promotes muscular regeneration through the ERK1/2 pathway. This study indicates that changes in butyrogenic bacteria and butyrate yield regulate sarcopenia development.

These results show that nutritional therapeutics, including ITF and fiber-enriched diet, may be integrated into the current exercise-based sarcopenia management. Besides, myoblast proproliferation and pathways involved provide new perspectives on preventing and treating age-specific skeleton muscle atrophy.

Conflicts of interest

There are no conflicts to declare.

Acknowledgements

The authors acknowledge the help of project coordinators, nurses and staff in patient assessments. The authors are thankful to Wenjia Qiu for her technical assistance with flow cytometry and kind encouragement.

Notes and references

1 S. Zhou, W. Zhang, G. Cai, Y. Ding, C. Wei, S. Li, Y. Yang, J. Qin, D. Liu, H. Zhang, X. Shao, J. Wang, H. Wang, W. Yang, H. Wang, S. Chen, P. Hu and L. Sun, *Cell Res.*, 2020, **30**, 1063–1077.

2 H. Sugihara, N. Teramoto, K. Nakamura, T. Shiga, T. Shirakawa, M. Matsuo, M. Ogasawara, I. Nishino, T. Matsuwaki, M. Nishihara and K. Yamanouchi, *Sci. Rep.*, 2020, **10**, 16385.

3 M. R. Islam, S. Arthur, J. Haynes, M. R. Butts, N. Nepal and U. Sundaram, *Nutrients*, 2022, **14**, 624.

4 E. E. Blaak, E. E. Canfora, S. Theis, G. Frost, A. K. Groen, G. Mithieux, A. Nauta, K. Scott, B. Stahl, J. van Harsselaar, R. van Tol, E. E. Vaughan and K. Verbeke, *Benefic. Microbes*, 2020, **11**, 411–455.
5 C. Martin-Gallausiaux, L. Marinelli, H. M. Blottiere, P. Larraufie and N. Lapaque, *Proc. Nutr. Soc.*, 2021, **80**, 37–49.
6 J. E. Moskowitz and S. Devkota, *Cell Host Microbe*, 2019, **26**, 574–576.
7 L. A. David, C. F. Maurice, R. N. Carmody, D. B. Gootenberg, J. E. Button, B. E. Wolfe, A. V. Ling, A. S. Devlin, Y. Varma, M. A. Fischbach, S. B. Biddinger, R. J. Dutton and P. J. Turnbaugh, *Nature*, 2014, **505**, 559–563.
8 G. den Besten, K. van Eunen, A. K. Groen, K. Venema, D. J. Reijngoud and B. M. Bakker, *J. Lipid Res.*, 2013, **54**, 2325–2340.
9 L. K. Brahe, A. Astrup and L. H. Larsen, *Obes. Rev.*, 2013, **14**, 950–959.
10 J. R. Davie, *J. Nutr.*, 2003, **133**, 2485S–2493S.
11 T. T. Song, X. Guan, X. Wang, S. S. Qu, S. W. Zhang, W. T. Hui, L. H. Men and X. Chen, *FASEB J.*, 2021, **35**, e21385.
12 M. E. Walsh, A. Bhattacharya, K. Sataranatarajan, R. Qaisar, L. Sloane, M. M. Rahman, M. Kinter and H. Van Remmen, *Aging Cell*, 2015, **14**, 957–970.
13 A. Ticinesi, A. Nouvenne, N. Cerundolo, P. Catania, B. Prati, C. Tana and T. Meschi, *Nutrients*, 2019, **11**, 1633.
14 J. H. Han, I. S. Kim, S. H. Jung, S. G. Lee, H. Y. Son and C. S. Myung, *PLoS One*, 2014, **9**, e95268.
15 E. E. Canfora, J. W. Jocken and E. E. Blaak, *Nat. Rev. Endocrinol.*, 2015, **11**, 577–591.
16 Z. G. Gao, J. Yin, J. Zhang, R. E. Ward, R. J. Martin, M. Lefevre, W. T. Cefalu and J. P. Ye, *Diabetes*, 2009, **58**, 1509–1517.
17 J. Frampton, K. G. Murphy, G. Frost and E. S. Chambers, *Nat. Metab.*, 2020, **2**, 840–848.
18 A. J. Brown, S. M. Goldsworthy, A. A. Barnes, M. M. Eilert, L. Tcheang, D. Daniels, A. I. Muir, M. J. Wigglesworth, I. Kinghorn, N. J. Fraser, N. B. Pike, J. C. Strum, K. M. Steplewski, P. R. Murdock, J. C. Holder, F. H. Marshall, P. G. Szekeres, S. Wilson, D. M. Ignar, S. M. Foord, A. Wise and S. J. Dowell, *J. Biol. Chem.*, 2003, **278**, 11312–11319.
19 N. C. Jones, Y. V. Fedorov, R. S. Rosenthal and B. B. Olwin, *J. Cell. Physiol.*, 2001, **186**, 104–115.
20 P. Wiedmer, T. Jung, J. P. Castro, L. C. D. Pomatto, P. Y. Sun, K. J. A. Davies and T. Grune, *Ageing Res. Rev.*, 2021, **65**, 101200.
21 M. R. Smith, F. Saad, B. Egerdie, P. R. Sieber, T. L. Tammela, C. Ke, B. Z. Leder and C. Goessl, *J. Clin. Oncol.*, 2012, **30**, 3271–3276.
22 K. Norman, U. Hass and M. Pirlich, *Nutrients*, 2021, **13**, 2764.
23 F. Q. Chen, S. Xu, Y. F. Wang, F. Chen, L. Cao, T. T. Liu, T. Huang, Q. Wei, G. J. Ma, Y. H. Zhao and D. F. Wang, *J. Diabetes Res.*, 2020, **2020**, 3950404.
24 A. Riviere, M. Selak, D. Lantin, F. Leroy and L. De Vuyst, *Front. Microbiol.*, 2016, **7**, 979.
25 A. Ticinesi, F. Lauretani, C. Milani, A. Nouvenne, C. Tana, D. Del Rio, M. Maggio, M. Ventura and T. Meschi, *Nutrients*, 2017, **9**, 1303.
26 M. J. Claesson, I. B. Jeffery, S. Conde, S. E. Power, E. M. O'Connor, S. Cusack, H. M. B. Harris, M. Coakley, B. Lakshminarayanan, O. O'Sullivan, G. F. Fitzgerald, J. Deane, M. O'Connor, N. Harnedy, K. O'Connor, D. O'Mahony, D. van Sinderen, M. Wallace, L. Brennan, C. Stanton, J. R. Marchesi, A. P. Fitzgerald, F. Shanahan, C. Hill, R. P. Ross and P. W. O'Toole, *Nature*, 2012, **488**, 178–185.
27 M. Jackson, I. B. Jeffery, M. Beaumont, J. T. Bell, A. G. Clark, R. E. Ley, P. W. O'Toole, T. D. Spector and C. J. Steves, *Genome Med.*, 2016, **8**, 21.
28 M. Vital, A. C. Howe and J. M. Tiedje, *mBio*, 2014, **5**, e00889.
29 P. Louis and H. J. Flint, *FEMS Microbiol. Lett.*, 2009, **294**, 1–8.
30 D. S. Han, W. K. Wu, P. Y. Liu, Y. T. Yang, H. C. Hsu, C. H. Kuo, M. S. Wu and T. G. Wang, *Clin. Nutr.*, 2022, **41**, 1491–1500.
31 C. A. Phillips, B. J. Reading, M. Livingston, K. Livingston and C. M. Ashwell, *Front. Physiol.*, 2020, **11**, 101.
32 S. Ustanina, J. Carvajal, P. Rigby and T. Braun, *Stem Cells*, 2007, **25**, 2006–2016.
33 J. L. Plank, M. T. Suflita, C. L. Galindo and P. A. Labosky, *Stem Cell Res.*, 2014, **12**, 233–240.
34 M. H. Jafferali, R. A. Figueroa, M. Hasan and E. Hallberg, *Sci. Rep.*, 2018, **8**, 4348.
35 C. Elabd, W. Cousin, P. Upadhyayula, R. Y. Chen, M. S. Chooljian, J. Li, S. Kung, K. P. Jiang and I. M. Conboy, *Nat. Commun.*, 2014, **5**, 4082.
36 S. F. Liu, F. Gao, L. Wen, M. Ouyang, Y. Wang, Q. Wang, L. P. Luo and Z. J. Jian, *Cell. Physiol. Biochem.*, 2017, **43**, 1100–1112.
37 S. Chiappalupi, G. Sorci, A. Vukasinovic, L. Salvadori, R. Sagheddu, D. Coletti, G. Renga, L. Romani, R. Donato and F. Riuzzi, *J. Cachexia, Sarcopenia*, 2020, **11**, 929–946.
38 J. D. Bernet, J. D. Doles, J. K. Hall, K. K. Tanaka, T. A. Carter and B. B. Olwin, *Nat. Med.*, 2014, **20**, 265–271.
39 J. Pu, G. Peng, L. H. Li, H. M. Na, Y. B. Liu and P. S. Liu, *J. Lipid Res.*, 2011, **52**, 1319–1327.
40 N. T. Baxter, A. W. Schmidt, A. Venkataraman, K. S. Kim, C. Waldron and T. M. Schmidt, *mBio*, 2019, **10**, e02566-18.
41 T. T. T. Tran, F. J. Cousin, D. B. Lynch, R. Menon, J. Brulc, J. R. M. Brown, E. O'Herlihy, L. F. Butto, K. Power, I. B. Jeffery, E. M. O'Connor and P. W. O'Toole, *Microbiome*, 2019, **7**, 39.